https://doi.org/10.5194/acp-2020-760
Preprint. Discussion started: 31 August 2020

Atmospheric Chemistry and Physics Discussions

Improvement of inorganic aerosol component in $PM_{2.5}$ by constraining aqueous-phase formation of sulfate in cloud with satellite retrievals: WRF-Chem simulations

Tong Sha[1], Xiaoyan Ma[1*], Jun Wang[2], Rong Tian[1], Jianqi Zhao[1], Fang Cao[3], Yan-Lin Zhang[3]

[1] Collaborative Innovation Center on Forecast and Evaluation of Meteorological Disasters (CIC-FEMD)/Key Laboratory for Aerosol-Cloud-Precipitation of China Meteorological Administration, Nanjing University of Information Science & Technology, Nanjing 210044, China

[2] Department of Chemical and Biochemical Engineering/Center for Global and Regional Environmental Research, The University of Iowa, Iowa City, IA, USA

[3] Yale–NUIST Center on Atmospheric Environment, International Joint Laboratory on Climate and Environment Change (ILCEC)/Jiangsu Provincial Key Laboratory of Agricultural Meteorology, College of Applied Meteorology, Nanjing University of Information Science & Technology, Nanjing 210044, China

https://doi.org/10.5194/acp-2020-760
Preprint. Discussion started: 31 August 2020

Atmospheric Chemistry and Physics Discussions

Abstract

High concentrations of $PM_{2.5}$ in China have caused severe visibility degradation and health problem. However, it is still a big challenge to accurately predict $PM_{2.5}$ and its chemical components in the numerical model. In this study, we compared the inorganic aerosol components of $PM_{2.5}$ (sulfate, nitrate, and ammonium (SNA)) simulated by WRF-Chem with in-situ data during a heavy haze-fog event (November 2018) in Nanjing. The comparisons show that the model underestimates the sulfate concentrations by 81 % and fails to reproduce the significant increase of sulfate concentrations from early morning to noon, which corresponds to the timing of fog dissipation, suggesting that the model underestimates the aqueous-phase formation of sulfate in clouds. In addition, the model overestimates both nitrate and ammonium concentrations by 184 % and 57 %, respectively. These ultimately result in the simulated SNA 77.2 % higher than the observations. However, as the important aqueous-phase reactors, cloud water are simultaneously underestimated by the model. Therefore, the modeled cloud water was constrained based on the MODIS Liquid Water Path (LWP) observations. Results show that the simulation with MODIS-corrected cloud water amount increases the sulfate by a factor of 3, decreases NMB by 53.5 %, and can reproduce its diurnal cycles, i.e. the peak concentration at noon. Also, the model absolute bias of nitrate decreases from 184 % to 50 %, especially for the nocturnal concentrations, which suggests the MODIS-constrained simulation improved the diurnal pattern. Although the simulated ammonium is still higher than the observation, corrected cloud water lead to the decrease of the modeled bias of SNA from 77.2 % to

https://doi.org/10.5194/acp-2020-760
Preprint. Discussion started: 31 August 2020

Atmospheric Chemistry and Physics Discussions

14.1 %. The strong sensitivity of simulated SNA concentration to the cloud water provides an explanation for the bias of SNA simulation. Hence, the uncertainties of cloud water can lead to model bias in simulating SNA, and can be reduced by constraining the model with satellite observations.

https://doi.org/10.5194/acp-2020-760
Preprint. Discussion started: 31 August 2020

Atmospheric Chemistry and Physics Discussions

1 Introduction

Severe and persistent haze pollution with daily concentrations of $PM_{2.5}$ exceeding the Chinese standard of 75 μg m^{-3}, occurs frequently in China during recent decades, which has aroused wide public attention due to its adverse impact on air quality, regional and global climate, and human health (Huang et al., 2014). According to previous studies, stagnant meteorological conditions with high atmospheric relative humidity and low boundary layer height, high emissions of primary air pollutants, as well as the rapid formation of secondary inorganic aerosols, including sulfate, nitrate, and ammonium (SNA), are considered to be the main factors leading to the haze episodes (Liu et al., 2020a). Earlier studies showed that the contribution of SNA to total $PM_{2.5}$ mass concentration was over 50% during the severe haze events (Cheng et al., 2016; Xu et al., 2017; Wang et al., 2019).

The chemical transport models (CTMs) are often used to predict the $PM_{2.5}$ pollution and evaluate the emission control strategies. Most models show reasonable performance on simulating surface $PM_{2.5}$ concentrations in China but perform poorly on simulating the proportion of chemical components in $PM_{2.5}$, especially during the severe haze periods (Gao et al., 2018; Chen et al., 2019). Many recent studies have reached an agreement that CTMs generally underestimate sulfate concentrations but overestimate nitrate concentrations (Wang et al., 2013; Wang et al., 2014; Zheng et al., 2015a; Chen et al., 2016; Cheng et al., 2016; Fu et al., 2016; Gao et al., 2016; Li et al., 2018a; Chen et al., 2019; Sha et al., 2019). The uncertainties such as meteorological fields (Bei et al., 2017; Li et al., 2017c; Su et al., 2018), emission inventories (Ma et al.,

https://doi.org/10.5194/acp-2020-760
Preprint. Discussion started: 31 August 2020


Atmospheric Chemistry and Physics Discussions

2018; Zhang et al., 2018; Qu et al., 2019), and parameterizations of physical and chemical processes in the model (Gao et al., 2018; Luo et al., 2019; Alexander et al., 2020), can contribute to the discrepancies of SNA and $PM_{2.5}$ between the models and observations.

The underestimation of sulfate in the models has been mainly attributed to the incomplete and/or inaccurate chemical mechanism. Generally, sulfate is formed through the gas-phase oxidation of SO_2 by OH radicals, and aqueous-phase oxidation of S(IV) ($= SO_2 \cdot H_2O + HSO_3^- + SO_3^{2-}$) by various oxidants (e.g., H_2O_2, O_3, NO_2, and O_2 (transition-metal-ion (TMI) catalysis)) in cloud droplets and aerosol water (the latter often called the heterogenous reaction) (Cheng et al., 2016; Liu et al., 2020a). It is worth noting that high atmospheric RH facilitates sulfate formation and aggravates the haze pollution (Xue et al., 2016; Tie et al., 2017; Wu et al., 2019). Therefore, the formation of sulfate is mainly through gas-phase reactions under relatively low atmospheric RH (RH < 30 %), but through heterogeneous and aqueous-phase reactions under relatively high atmospheric RH (RH > 60 %) (Li et al., 2017a). However, the mechanisms of sulfate formation at high RH is still controversial and unclear (Cheng et al., 2016; Wang et al., 2016; Ge et al., 2017; Guo et al., 2017; Liu et al., 2017; Yang et al., 2017; Li et al., 2018b). Previous studies proposed that the oxidation of SO_2 by NO_2 in aerosol water with almost neutral aerosol pH values (5.4-7.0) plays a dominant role in sulfate formation during the severe haze episodes (Cheng et al., 2016; Wang et al., 2016). However, the aerosol pH calculated by the ISORROPIA II model was moderately acidic with the value of 3.0-4.9, suggesting that the pathway of SO_2 oxidation by dissolved

https://doi.org/10.5194/acp-2020-760
Preprint. Discussion started: 31 August 2020


Atmospheric Chemistry and Physics Discussions

NO_2 was not important during the haze events in China (Guo et al., 2017; Ding et al., 2019). Latest studies suggested that SO_2 heterogeneous reaction via TMI-catalyzed oxidation perhaps dominates the sulfate formation during the haze periods, which is also verified by the observations of sulfate oxygen isotopes (Shao et al., 2019). Since the observations of the concentration, complexation, and solubility of TMI are not available, the mechanism still remains unclear (Jacob, 2000; Wang et al., 2020). In order to tackle the underestimation of sulfate in the model during the haze events, most studies add the SO_2 heterogeneous reaction in the model, which is usually parameterized as a reactive uptake process and assumed to be irreversible (Wang et al., 2014; Zheng et al., 2015b; Chen et al., 2016; Li et al., 2017a; Feng et al., 2018; Li et al., 2018a; Sha et al., 2019; Shao et al., 2019). Although the implementation of SO_2 heterogeneous reactions in the model can achieve an agreement of simulated and observed sulfate concentrations during the haze episodes, the model still underestimates the sulfate due to uncertainties of the parameters in this reaction, such as the pH, water content and surface area of aerosol, as well as the gas uptake coefficients on aerosol water.

Cloud/fog droplets can act as efficient reactors in which dissolved SO_2 reacts with oxidations to form sulfate. Many studies showed that sulfate concentrations would be enhanced by the occurrence of cloud and fog compared to the cloud-free conditions (Crahan et al., 2004; Sorooshian et al., 2006; 2007; Wonaschuetz et al., 2012; Ervens et al., 2018a). Previous modeling studies concluded that a major fraction of sulfate (60-90%) is formed via aqueous (in-cloud) chemistry globally (Barth et al., 2000; Ma and

https://doi.org/10.5194/acp-2020-760
Preprint. Discussion started: 31 August 2020


Atmospheric Chemistry and Physics Discussions

Salzen, 2006; Harris et al., 2013; Kim et al., 2015; Ervens et al., 2018b; Dovrou et al., 2019). The aqueous formation rate depends on liquid water content (LWC), the size distribution, pH and lifetime of cloud droplets, as well as the availability of oxidants. The kinetic and mechanistic parameters that characterize the uptake processes of sulfate precursors and oxidants, as well as the chemical reactions leading to sulfate formation in the aqueous phase, are relatively well constrained in the model, therefore the largest uncertainties in predicting in-cloud sulfate formation do not originate from the understanding of the chemical processes, but from the prediction of cloud microphysical and dynamical parameters, such as LWC and cloud lifetime (Rasch et al., 2000; Ervens et al., 2015). Mueller et al. (2006) found that the simulated sulfate concentration significantly increased after correcting the underestimation of model cloud fraction. Xie et al. (2019) showed that the improvement in cloud fields in MERRA-2 can eliminate approximately half of the bias in the surface sulfate concentration during summertime relative to the MERRA data. However, only a few studies focus on the sulfate underestimation caused by the bias of cloud fields during the haze episodes. Therefore, a better understanding of the sensitivity of sulfate simulations to cloud water is needed to improve the model performance on predicting $PM_{2.5}$.

A persistent high $PM_{2.5}$ level accompanying the fog event (short as haze-fog event) occurred in the Yangtze River Delta from 26 October to 2 December 2018. We choose this period to investigate the impact of cloud/fog water on simulating SNA using the WRF-Chem Model. The paper is organized as below. Section 2 shows the descriptions

https://doi.org/10.5194/acp-2020-760
Preprint. Discussion started: 31 August 2020


Atmospheric Chemistry and Physics Discussions

of the model and data, as well as the meteorology evaluation. The evaluation of simulated chemical fields and cloud water with observations, and sensitivity experiments to study the impact of corrected cloud water on simulated SNA are presented in section 3 and 4. Section 5 shows the summaries.

2 Model configurations, data description, and model evaluation

2.1 Model configurations

The WRF-Chem version 3.9.1 (Grell et al., 2005) is used in this study to conduct the simulations on a domain over the eastern China with the horizontal resolution of 27 km and nested to a domain with 9 km covering the YRD (Fig. 1(a)). There are 42 vertical levels, with 24 levels below the boundary layer (about 1500 m) and the lowest level about 21 m. The physical parameterization schemes include Lin microphysical scheme (Chen and Sun, 2002), Grell 3-D cumulus scheme (Grell and Dezső, 2002), RRTM (Mlawer et al., 1997) for longwave radiation and Goddard scheme for shortwave radiation (Chou and Suarez, 1994), Yonsei University planetary boundary layer parameterization (Hong et al., 2006), QNSE surface layer scheme (Sukoriansky et al., 2005) and Noah land surface model (Tewari et al., 2004).

The Carbon Bond Mechanism (CBMZ) for gas-phase chemistry (Zaveri and Peters, 1999) and Model for Simulating Aerosol Interactions and Chemistry (MOSAIC) aerosol module with 4 sectional aerosol bins and aqueous reactions (Zaveri et al., 2008) are chosen in our study. MOSAIC predicts all the major aerosol species, including sulfate, nitrate, ammonium, BC, primary organic mass, chloride, sodium, other inorganic mass (OIN), and liquid water. Detailed descriptions of the SNA formation

https://doi.org/10.5194/acp-2020-760
Preprint. Discussion started: 31 August 2020


Atmospheric Chemistry and Physics Discussions

mechanisms in the standard model can be found in Sha et al. (2019).

The 0.25°×0.25° National Center for Environmental Prediction's (NCEP) Final Analysis (FNL) dataset (http://rda.ucar.edu/datasets/ds083.2/) provides the meteorological initial and boundary condition. Anthropogenic emissions are taken from Multi-resolution Emission Inventory for China (MEIC: http://www.meicmodel.org/) for the year 2016 (Li et al., 2017b). The simulation starts on 24 November and ends on 2 December 2018, with the first 48 hours as the spin-up period.

2.2 Observational data

Meteorological variables are measured every three hours from five weather stations in Nanjing, and obtained for this study from the Meteorological Information Comprehensive Analysis and Process System (MICAPS) (green triangles in Fig. 1(b)), which are used to evaluate the model performance on simulating meteorological fields. The data include air temperature and relative humidity at 2m (T2, RH), wind speed and direction at 10m (WS10, WD10), visibility (VIS), and accumulated precipitation (PRE) (only the sample frequency of precipitation is 6 hourly). For surface pollution, two data sets are used: (1) the hourly SO_2, NH_3, HNO_3, HONO, and inorganic chemical components in $PM_{2.5}$ (sulfate, nitrate, and ammonium) concentrations measured by the In-situ Gas and Aerosol Compositions monitor (IGAC) (Young et al., 2016) at Nanjing University of Information Science & Technology (NUSIT) (32.2º N, 118.7º E; 22m above sea level) (the blue circle in Fig. 1(b)); (2) the routine measurements of hourly NO_2 and $PM_{2.5}$ concentrations at Maigaoqiao monitoring site (32.1º N, 118.8º E) in Nanjing from the China National Environmental Monitoring Center (CNEMC) (since

https://doi.org/10.5194/acp-2020-760
Preprint. Discussion started: 31 August 2020


Atmospheric Chemistry and Physics Discussions

the NUIST site did not observe NO_2 and $PM_{2.5}$ simultaneously, the observation data from Maigaoqiao site nearest to the NUIST were used, shown as the red circle in Fig. 1(b)). Himawari 8 satellite data are used to represent the spatial area of this fog event (https://www.eorc.jaxa.jp/ptree/index.html). Fog area is mainly indicated by the albedo at three visible bands: red (band 3, 0.64 μm), green (band 2, 0.51 μm) and blue (band 1, 0.47 μm). Finally, the daily liquid water path (LWP) observations from the MODIS Aqua Collection 6 Level-3 production are used to evaluate the model performance on simulating cloud water.

2.3 Model evaluation

Comparisons between the simulated and observed meteorological parameters from 26 October to 2 December 2018 in Nanjing are shown in Fig. 2. The model can reproduce the temporal variation of observed meteorological variables, such as T2, RH, WS10, and WD10, with the relatively high correlations of 0.89, 0.68, 0.47 and 0.55, and small root-mean-square errors (RMSEs) of 1.7 °C, 9.7 %, 0.6 m s^{-1} and 61.7°, respectively. The simulated T2, RH, and WS10 are slightly lower than observations, with the mean biases of -0.4 °C, -1.4 %, and -0.1 m s^{-1}, respectively (Table 2). There was almost no precipitation during this period. Similarly, the simulated precipitation is also quite limited except for the date on 2 December. Overall, the simulated meteorological fields are reasonable in Nanjing.

3 Results and discussions

3.1 Chemical simulations

From 26 November to 2 December 2018, Nanjing and its surrounding cities

https://doi.org/10.5194/acp-2020-760
Preprint. Discussion started: 31 August 2020


Atmospheric Chemistry and Physics Discussions

suffered from a severe haze-fog event for seven days (fog areas are shown in Fig. S1). The average $PM_{2.5}$ concentrations and RH in Nanjing exceeded 115 μg m^{-3} and 85%, respectively, and the visibility is less than 50 meters in some areas.

The hourly and diurnal variations of simulated and observed SO_2, NO_2, NH_3, HNO_3, and HONO as well as SNA and $PM_{2.5}$ concentrations are shown in Fig. 3 and 4. The magnitudes and temporal variations of air pollutants from the simulations and observations are generally consistent. However, the model overestimates SO_2 by 114 % and underestimates sulfate by over 80 %, and thus underestimates the sulfur oxidation ratio (SOR) by 81 %. A low oxidation rate of SO_2 to sulfate in the model has been found in previous studies (Gao et al., 2018). Possible explanations are probably associated with unclear or imperfect chemical mechanisms of sulfate formation in the models. (Moch et al., 2018; Sha et al., 2019; Shao et al., 2019). Additionally, it is noted that the observed sulfate concentration has an obvious diurnal cycle with the peak occurring at noon, corresponding to the timing of fog dissipation. Sulfate mass concentration can remain at a relatively high level in fog water during the night and early morning due to the contribution from aqueous chemistry, inducing a significant increase of sulfate when fog droplets evaporate at noon (Xue et al., 2016). However, the simulated sulfate shows a flatter diurnal cycle, with a much smaller concentration enhancement rate (0.45 μg m^{-3} hr^{-1}) from early morning to noon compared to the observations (2.3 μg m^{-3} hr^{-1}), suggesting that model possibly underestimates the formation of sulfate via aqueous-phase chemistry in clouds.

Globally, the aqueous sulfate formation is mainly from the oxidation of S(IV) by

https://doi.org/10.5194/acp-2020-760
Preprint. Discussion started: 31 August 2020


Atmospheric Chemistry and Physics Discussions

H_2O_2 and O_3, and almost 50% from the oxidation by H_2O_2. Previous studies indicated that the heavy pollution in China is usually associated with a weak photochemical activity, while the formation of atmospheric oxidant species (e.g. OH, H_2O_2, and O_3) is driven by photolysis, which could suppress the formation of sulfate via the oxidation of S(IV) by H_2O_2 and O_3 during the haze-fog events (Xue et al., 2016; Li et al., 2017a; Wang et al., 2020; Liu et al., 2020b). Therefore, the aqueous-phase oxidations of S(IV) by NO_2 and O_2 (TMI-catalyzed) could play an important role in sulfate formation. It is noted that the observed HONO concentrations rise remarkably at noon, which is quite consistent with the diurnal cycle of sulfate (Fig. 4(b, g)), while most of the HONO is produced via SO_2 oxidation by NO_2 in aqueous phase according to previous studies (Liu et al., 2019). It is therefore suggested that the aqueous-phase oxidations of S(IV) by NO_2 is possibly the main pathway of sulfate formation during this haze-fog event. However, the simulated HONO is almost an order of magnitude lower than the observations and has no obvious diurnal variations as shown in the observations.

Although the diurnal pattern of NO_2 is consistent in the model and observations, and the averaged NMB is only 12 %, the nitrate concentrations are 184 % higher in the model than in the observations, especially at night, suggesting that the model overestimates the nitrate nocturnal formation pathway, that is, the N_2O_5 heterogeneous hydrolysis uptake on the surfaces of deliquescence aerosols (Lowe et al., 2015; Brown et al., 2016; Chang et al., 2016). The relatively high N_2O_5 uptake coefficient (γ_{N2O5}) and missing of heterogeneous production of nitryl chloride ($ClNO_2$) from the N_2O_5 uptake on chloride aerosols in the model, lead to the overestimation of the simulated nitrate

https://doi.org/10.5194/acp-2020-760
Preprint. Discussion started: 31 August 2020


Atmospheric Chemistry and Physics Discussions

mass concentration (Sarwar et al., 2012, 2014; McDuffie et al., 2018). Besides, overestimations of the HNO_3 and nitrate ($TNO_3 = HNO_3 + NO_3^-$) concentrations in the model are also caused by the insufficient removal of TNO_3. Therefore, too much TNO_3 may consume a large amount of NH_3 to a certain extent, further inhibit the sulfate formation.

The molar concentrations of total ammonium ($TNH_4 = NH_3 + NH_4^+$) are generally consistent in the simulations and observations, i.e. 2.1 mol m^{-3} in the simulation and 2.5 mol m^{-3} in the observation, but the simulated NH_3 is 91 % lower and ammonium is 57 % higher than the observations (Fig. 3(e, f)). This is partly due to the overestimation of TNO_3 in the model (Wang et al., 2013). On the other hand, aerosol acidity is a key factor driving the semi-volatile partitioning of aerosol species, and lower aerosol pH is conducive to the existence of ammonium in the particle phase. As shown in Fig. S2, the model underestimates aerosol pH by 0.8, which leads to the discrepancies of TNH_4 gas-particle partitioning.

The simulated $PM_{2.5}$ concentrations are significantly higher than the observations (twice during daytime and three times during night). As CBMZ-MOSAIC only predicts primary organic species but does not consider the formation of secondary organic aerosol, the organic mass concentration must assumedly be underestimated in the model. Therefore, the overestimation of $PM_{2.5}$ is mainly due to the overestimation of SNA, namely nitrate and ammonium. Additionally, the overestimation of primary inorganic aerosols mass concentrations in the model can also lead to a positive bias of $PM_{2.5}$.

3.2 Cloud water

https://doi.org/10.5194/acp-2020-760
Preprint. Discussion started: 31 August 2020


Atmospheric Chemistry and Physics Discussions

Based on the above analysis, we speculated that underestimation of sulfate in the model is due to the insufficient in-cloud aqueous-phase formation and/or missing mechanisms in the model. The cloud water is the most uncertain factor to modulate in-cloud aqueous-phase chemistry (Ervens et al., 2015; Xie et al., 2018). Therefore, it is necessary to evaluate the simulated cloud water in the model.

Figure 5 shows the spatial distribution of simulated fog from 26 November to 2 December over YRD. The fog area was identified once LWP is above a threshold of 2 g m^{-2} (Jia et al., 2019). The model can generally reproduce the distribution characteristics of the fog area observed at 08:00 every day during this period, except for the date on 27 November (the observed fog areas are shown in Fig. S1).

The LWC at the lowest level of the model has an important impact on the SNA formation at surface. LWC was not observed simultaneously during this period, so visibility (VIS) is usually used to assess the simulated LWC as it is a function of LWC and cloud droplet number (N_c) (Eq. (1); Gultepe et al., 2006).

$$\mathrm{VIS[m]} = 1002/(\mathrm{LWC[g\ cm^{-3}]} \times \mathrm{N_c[cm^{-3}]}^{0.6473}) \quad (1)$$

Figure 6 compares the spatial distribution of VIS from simulations and observations (threshold of VIS < 1000 m). The simulated VIS has similar spatial pattern and magnitude with the observed VIS. However, the model tends to overestimate VIS, especially on 27 November, likely because the LWC is underestimated. The underestimation of LWC during this period may be related to the bulk microphysical scheme used in the model (Khain et al., 2009; Jia et al., 2019).

To quantitatively evaluate the modeled cloud water, we compared the simulated

https://doi.org/10.5194/acp-2020-760
Preprint. Discussion started: 31 August 2020


Atmospheric Chemistry and Physics Discussions

LWP with the MODIS daily observation (Fig. 7). The model can reproduce the spatial distribution of observed LWP but somewhat underestimates LWP in some areas, e.g. Jiangsu Province. Comparisons of the cumulative probability distribution of the simulated and observed LWP are shown in Fig. 8. The probability distribution of the simulated LWP is mainly concentrated in the lower LWP, e.g. the probability of the simulated LWP less than 20 g m^{-2} is ~ 80 %, while the observed one is only 30 % (Table 2). The modeled probabilities are 49 % lower than the observed ones for larger LWP (> 20 g m^{-2}). The results are consistent with previous studies (Mueller et al., 2006; Kay et al., 2012; Wang et al., 2013; Sha et al., 2019).

As stated above, the model underestimates the sulfate mass concentration and cloud water simultaneously during the haze-fog event. The underestimation of cloud water possibly leads to the insufficient contribution of in-cloud aqueous-phase chemistry to sulfate formation, which could explain the underestimation of sulfate during the haze episode, but has been overlooked by most previous studies. Therefore, the next section uses the observed LWP from MODIS to constrain the simulations and explore the impact of cloud water on SNA simulation.

3.3 Sensitivity experiments

3.3.1 Constrain of cloud water in the model

The logarithmic function is used to fit the cumulative probability distributions (CPD) for both the observed and simulated LWP (Fig. 8) values. The corresponding equations of the fitting are:

$$F_o = -6.4 + 16.5\ln(x_o + 1.0) \qquad (0 \le x_o \le 500\ \mathrm{g\ m^{-2}}) \quad (2)$$

https://doi.org/10.5194/acp-2020-760
Preprint. Discussion started: 31 August 2020


Atmospheric Chemistry and Physics Discussions

$$F_{\mathrm{m}} = 59.1 + 6.7\ln(x_{\mathrm{m}} + 5.8) \qquad (0 \le x_{\mathrm{m}} \le 500\ \mathrm{g\ m^{-2}}) \quad (3)$$

Where subscripts o and m represent the observation and model, while *F* and *x* represent CPD and LWP. To update the modeled LWP with satellite observations, we use the histogram matching method (Richard, 2013), so that the CPD function of the simulated LWP after constraining is the same as the observations, i.e., $F_{\mathrm{m}}^{\mathrm{c}} = F_{\mathrm{o}}$. Consequently, the equation for transforming the modeled LWP is:

$$x_{\mathrm{m}}^{\mathrm{c}} = 53.0 \times (x_{\mathrm{m}} + 5.8)^{0.4} - 1 \qquad (4)$$

Where the subscript c presents the correction with MODIS observations.

We apply the Eq. (4) to modify the cloud water in the aqueous chemistry module only while cloud water amount in other modules (i.e. microphysics, cumulus parameterization, wet scavenging, and radiative transfer modules) remain unchanged to ensure that other physical and chemical processes are self-consistent between the control and sensitivity model simulations. This sensitivity experiment is called Sen_c. Consequently, the changes don't affect the cloud properties used in the radiative transfer calculations. As such, gas phase production rates are intact. However, cloud-induced changes in aqueous phase production do alter the mixing ratios of SO_2 and other oxidants (e.g., OH and H_2O_2), which could in turn impact the rate of gas phase oxidation. In addition, the changes in cloud water can affect the production rates of sulfate by changing the hydrogen ions concentrations ($[H^+]$). The pH of cloud water is considered as one of the important parameters affecting the aqueous-phase reaction rates. As shown in Fig. S3, constraining the simulated cloud water alone results in a decrease of cloud water pH (2.4) during this period. To eliminate the influence of changes in cloud water

https://doi.org/10.5194/acp-2020-760
Preprint. Discussion started: 31 August 2020


Atmospheric Chemistry and Physics Discussions

pH (from MODIS-based change of cloud water) on the sulfate production, we also increase the cloud water pH by 2 in another sensitivity experiment (Sen_c_pH) to make cloud water pH as close as possible to the control simulation. The experiment descriptions are shown in Table 3.

3.3.2 Impact of cloud constraint on SNA

Figure 9 shows the spatial distribution of the simulated SNA in the control and sensitivity simulations, as well as the difference between the two simulations. The simulated sulfate concentration in Sen_c_pH is 6 μg m^{-3} larger than the Control over the entire YRD, with the biggest difference in the south of Jiangsu and the east of Anhui province, corresponding to the area mostly affected by this haze-fog event (Fig. S1). It is indicated that corrected cloud water increases the contribution of the aqueous-phase chemistry to sulfate formation, thereby reducing the negative bias of simulated sulfate. The formation of sulfate greatly limits the nitrate production, so the simulated nitrate in Sen_c_pH is decreased by 35 μg m^{-3} compared to the Control over the entire YRD. However, the ammonium simulated by Sen_c_pH is larger than the results of Control run in most areas of YRD, with the average difference of 9 μg m^{-3}. As the inorganic aerosol system is essentially an acid-base titration, an increase in S(VI) concentration can neutralize more NH_3 to form ammonium sulfate ($(NH_4)_2SO_4$) or ammonium bisulfate (NH_4HSO_4), leading to an increase of simulated ammonium concentrations.

As shown in Fig. 10 and Fig. 11, Sen_c_pH significantly improves the simulation of sulfate, i.e. increases sulfate by 11.8 μg m^{-3} (295 %), and decreases NMB by 53.5 %. Also, the simulation using corrected cloud water can reproduce the diurnal cycle and

https://doi.org/10.5194/acp-2020-760
Preprint. Discussion started: 31 August 2020


Atmospheric Chemistry and Physics Discussions

capture the peak concentration of sulfate at noon, with the concentration increased rate of 1.8 μg m^{-3} hr^{-1} from early morning to noon, which is not seen in the Control run. Meanwhile, Sen_c_pH decreases the absolute bias of the simulated nitrate from 184.0% (Control) to 50.1 %, and greatly reduces the nitrate concentration at night, and thus predicts a better diurnal cycle. However, the simulation with corrected cloud water leads to a minor increase of ammonium.

Overall, the simulation with MODIS-corrected cloud water can obviously decrease the model bias of SNA to 14.1 % from 77.2 % in Control run (Fig. 11(a)). The proportion of sulfate in SNA also significantly increases from 2.5 % (Control) to 20.2 % (Sen_c_pH), which is much close to the observation (23.9 %), but still 6 μg m^{-3} lower than the observations. A few possibilities can explain the discrepancies. The model possibly underestimates the cloud water pH, with the value of 3.3 in Sen_c_pH (Fig. S4), which is relatively lower than the global typical cloud/fog water pH of 3-6 and the mean value of 4-6 suggested by Pye et al. (2020). The observed fog water pH in Nanjing from previous studies (Li et al., 2008; Lu et al., 2010; Qin et al., 2011; Yan et al., 2013; Hong et al., 2019) are summarized in Table 4, suggesting that the fog water pH in Nanjing is generally between 4.3 and 6.5. Therefore, the relatively lower fog water pH simulated by the model could limit the aqueous-phase formation of sulfate to some extent. Note that the aqueous-phase oxidation of S(IV) by NO_2 requires the cloud water pH of about 6, thus the more acidic cloud water in the model is not conducive to this reaction. Moreover, the model lacks SO_2 heterogeneous reactions on aerosol water (Li et al., 2017a; Shao et al., 2019) and other aqueous-phase reactions in clouds, such as

https://doi.org/10.5194/acp-2020-760
Preprint. Discussion started: 31 August 2020


Atmospheric Chemistry and Physics Discussions

the aqueous oxidation of S(IV) by HCHO and hydroxyl hydroperoxide (ISOPOOH) to form hydroxy-methane sulfonate (HMS) and sulfate (Moch et al., 2018; Dovrou et al., 2019), can also explain the sulfate underestimation even though the cloud water has already been corrected. In addition, cloud constraints are based on the MODIS LWP, which has been reported with an uncertainty range of ±30 % (Dong et al., 2008; Min et al., 2012; Khanal et al., 2018).

It should also be noted that compared to the observations, Sen_c_pH underestimates nitrate and overestimates ammonium in SNA (Fig. 11(b)), which can be ascribed to the underestimation of atmospheric acidity in the model, including the pH of aerosol and cloud/fog water. The hydrogen ion activity in aqueous aerosols can affect the partitioning of TNO_3 and TNH_4 between the gas and aerosol phases. Lower aerosol pH favors partitioning of TNO_3 toward gaseous HNO_3 rather than aerosol nitrate. In contrast, TNH_4 partitions toward gaseous NH_3 at higher aerosol pH (Weber et al., 2016). The simulated aerosol pH in Sen_c_pH is lower than the observations (Fig. S2), which is not conducive to the existence of aerosol nitrate. Additionally, because the scavenging efficiency of TNO_3 and TNH_4 is dependent upon cloud water pH, the acidic cloud water in the model can also cause these discrepancies.

4 Conclusions

Accurately predicting the concentrations and chemical components of particulate matter are still very challenging for climate and air quality models. In this study, we evaluated the WRF-Chem performance on simulating inorganic aerosol components of $PM_{2.5}$ during a haze-fog event in Nanjing, and investigate the possible reasons

https://doi.org/10.5194/acp-2020-760
Preprint. Discussion started: 31 August 2020


Atmospheric Chemistry and Physics Discussions

398 contributing to model bias in simulating SNA compared with the observations.

399 Our results presented that WRF-Chem overestimates SO_2 by 114 %,
400 underestimates sulfate by 81%, and fails to reproduce the diurnal cycle of sulfate, i.e.
401 the peak concentration at noon, which corresponds to the timing of fog dissipation. In
402 contrast, the model bias of NO_2 is much smaller (NMB = 12 %), but the nitrate is
403 overestimated by 184 %, especially its nocturnal concentration. Although the molar
404 concentrations of total ammonium are generally consistent in the simulations and
405 observations, the model underestimates NH_3 by 91 % and overestimates ammonium by
406 57%.

407 The underestimation of sulfate concentration is consistent with previous findings.
408 However, our work stands in contrast to previous studies that adding SO_2 heterogeneous
409 mechanism in the model to improve the simulation of sulfate. Cloud/fog droplets are
410 the important reactors in which dissolved SO_2 reacts with oxidations to form sulfate,
411 but the model underestimates cloud water (both surface LWC and LWP) simultaneously.
412 Therefore, the cloud water in the model was constrained based on the MODIS LWP
413 observations, and sensitivity experiments were conducted to explore the impact of
414 corrected cloud water on SNA simulation. Compare with control run, the simulation
415 with MODIS-corrected cloud water significantly improves the simulation of sulfate, i.e.
416 increases the concentration by nearly 3 times and decreases NMB by 53.5 %, as well
417 as reproduces the diurnal cycles. Additionally, corrected cloud water decreases the bias
418 of simulated nitrate by 134 %, especially the nocturnal concentrations, thus predicting
419 a better diurnal cycle. Although the simulated ammonium is higher than the control

https://doi.org/10.5194/acp-2020-760
Preprint. Discussion started: 31 August 2020


Atmospheric Chemistry and Physics Discussions

simulation and observation, corrected cloud water decreases the model bias of SNA to 14.1 % from 77.2 % (Control).

However, even after the MODIS-based adjustment of cloud water, the simulated sulfate is still 6 μg m^{-3} (27.5%) lower than the observations, suggesting that the model possibly underestimates the cloud water pH (the value of 3.3), which is not conducive to the in-cloud aqueous-phase oxidation of S(IV) by NO_2. Missing of SO_2 heterogeneous reactions on aerosol water (e.g., TMI-catalyzed oxidation) and other in-cloud aqueous-phase reactions (e.g., S(IV) oxidation by HCHO and ISOPOOH) in the model can also lead to underestimating the sulfate concentrations. In addition, the constraints of cloud water are based on the MODIS observations, which are themselves subject to retrieval uncertainties.

The above results emphasize the critical role of cloud water in simulating SNA, and provide a new perspective on the causes of sulfate underestimation discussed by the previous studies. More studies are still needed to comprehensively evaluate the modeled cloud fields to improve the haze prediction in the future.

Code and data availability: Some of the data repositories have been listed in Sect. 2. The other data, model outputs and codes can be accessed by contacting Tong Sha via shat@nuist.edu.cn.

Author contributions: TS performed the model simulation, data analysis and paper writing. XM proposed the idea, supervised this work and revised the paper. JW gave

https://doi.org/10.5194/acp-2020-760
Preprint. Discussion started: 31 August 2020


Atmospheric Chemistry and Physics Discussions

442 scientific suggestions and also contributed to the paper revision. RT processed the
443 observation data. JZ offered help with the model simulation. FC and YZ provided the
444 observation data at the NUIST site.

445

446 **Competing interests:** The authors declare that they have no conflict of interest.

447

448 **Acknowledgment:** This study is supported by the National Natural Science Foundation
449 of China grants (41675004 & 41975002), the National Key R&D Program of China
450 grants (2019YFA0606802 & 2016YFA0600404), and the Postgraduate Research &
451 Practice Innovation Program of Jiangsu Province (grant no. KYCX20_0919). Jun
452 Wang's participation of this project is made possible through in-kind support from the
453 University of Iowa.

https://doi.org/10.5194/acp-2020-760
Preprint. Discussion started: 31 August 2020

Atmospheric Chemistry and Physics Discussions

454 **Reference：**

455 Alexander, B., Sherwen, T., Holmes, C. D., Fisher, J. A., Chen, Q., Evans, M. J., and
456 Kasibhatla, P.: Global inorganic nitrate production mechanisms: comparison of a
457 global model with nitrate isotope observations, Atmos. Chem. Phys., 20, 3859-
458 3877, https://doi.org/10.5194/acp-20-3859-2020, 2020.

459 Barth, M. C., Rasch, P. J., Kiehl, J. T., Benkovitz, C. M., Schwartz, S. E.: Sulfur
460 chemistry in the national center for atmospheric Research community climate
461 model: description, evaluation, features and sensitivity to aqueous chemistry, J.
462 Geophys. Res. Atmos., 105, 1387–1415, 2000.

463 Bei, N. F., Wu, J. R., Elser, M., Feng, T., Cao, J. J., El-Haddad, I., Li, X., Huang, R. J.,
464 Li, Z. Q., Long, X., Xing, L., Zhao, S. Y., Tie, X. X., Prevot, A. S. H., and Li, G.
465 H.: Impacts of meteorological uncertainties on the haze formation in Beijing-
466 Tianjin-Hebei (BTH) during wintertime: a case study, Atmos. Chem. Phys., 17,
467 14579-14591, https://doi.org/10.5194/acp-17-14579-2017, 2017.

468 Brown, S. S., Dubé, W. P., Tham, Y. J., Zha, Q., Xue, L., Poon, S., Wang, Z., Blake, D.
469 R., Tsui, W., Parrish, D. D., Wang, T.: Nighttime chemistry at a high altitude site
470 above Hong Kong, J. Geophys. Res. 121, 2457–2475.
471 https://doi.org/10.1002/2015JD024566, 2016.

472 Chang, W. L., Brown, S. S., Stutz, J., Middlebrook, A. M., Bahreini, R., Wagner, N. L.,
473 Dubé, W. P., Pollack, I. B., Ryerson, T. B., Riemer, N.: Evaluating N2O5
474 heterogeneous hydrolysis parameterizations for CalNex 2010, J. Geophys. Res.
475 121, 5051–5070. https://doi.org/10.1002/2015JD024737, 2016.

https://doi.org/10.5194/acp-2020-760
Preprint. Discussion started: 31 August 2020

476 Chen, D., Liu, Z. Q., Fast, J., Ban, J. M.: Simulations of sulfate–nitrate–ammonium
477 (SNA) aerosols during the extreme haze events over northern China in October
478 2014, Atmos. Chem. Phys., 16 (16), 10707-10724, 2016.
479 Chen, L., Gao, Y., Zhang, M., Fu, J. S., Zhu, J., Liao, H., Li, J., Huang, K., Ge, B.,
480 Wang, X., Lam, Y. F., Lin, C. Y., Itahashi, S., Nagashima, T., Kajino, M., Yamaji,
481 K., Wang, Z., and Kurokawa, J.: MICS-Asia III: multi-model comparison and
482 evaluation of aerosol over East Asia, Atmos. Chem. Phys., 19, 11911-11937,
483 https://doi.org/10.5194/acp-19-11911-2019, 2019.
484 Chen, S. H. and Sun W. Y.: A one-dimensional time dependent cloud model, J. Meteor.
485 Soc. Japan., 80(1), 99–118. doi:10.2151/jmsj.80.99, 2002.
486 Cheng, Y. F., Zheng, G. J., Wei, C., Mu, Q., Zheng, B., Wang, Z. B., Gao, M., Zhang,
487 Q., He, K. B., Gregory, R. C., Ulrich, P., Su, H.: Reactive nitrogen chemistry in
488 aerosol water as a source of sulfate during haze events in China, Sci. Adv. 2 (12)
489 1601530- 1601530, 2016.
490 Chou, M. D., and Suarez, M. J.: An efficient thermal infrared radiation parameterization
491 for use in general circulation models, NASA Tech. Memo., 104606, 3, 85pp, 1994.
492 Crahan, K. K., Hegg, D., Covert, D. S., and Jonsson, H.: An exploration of aqueous
493 oxalic acid production in the coastal marine atmosphere, Atmos. Environ., 38,
494 3757–3764, https://doi.org/10.1016/j.atmosenv.2004.04.009, 2004.
495 Ding, J., Zhao, P., Su, J., Dong, Q., Du, X., and Zhang, Y.: Aerosol pH and its driving
496 factors in Beijing, Atmos. Chem. Phys., 19, 7939–7954,
497 https://doi.org/10.5194/acp-19-7939-2019, 2019.

https://doi.org/10.5194/acp-2020-760
Preprint. Discussion started: 31 August 2020

Atmospheric Chemistry and Physics Discussions

498 Dong, X. Q., Minnis, P., Xi, B., Sun-Mack, S., Chen, Y.: Comparison of CERES-
499 MODIS stratus cloud properties with ground-based measurements at the DOE
500 ARM Southern Great Plains site, J. Geophys. Res. Atmos., 113, D03204.
501 https://doi.org/10.1029/ 2007JD008438, 2008.
502 Dovrou, E., Rivera-Rios, J. C., H. Bates, K., and N. Keutsch, F.: Sulfate Formation
503 via Cloud Processing from Isoprene Hydroxyl Hydroperoxides (ISOPOOH),
504 Environ. Sci. Technol., 53, 12476−12484, 2019.
505 Ervens, B., Sorooshian A., M. Aldhaif, A., Shingler, T., Crosbie, E., Ziemba, L.,
506 Campuzano-Jost, P., Jimenez, J. L., and Wisthaler, A.: Is there an aerosol signature
507 of chemical cloud processing? Atmos. Chem. Phys., 18, 16099–16119,
508 https://doi.org/10.5194/acp-18-16099-2018, 2018a.
509 Ervens, B.: Modeling the processing of aerosol and trace gases in clouds and fogs,
510 Chem. Rev., 115(10), 4157-4198, 2015.
511 Ervens, B.: Progress and Problems in Modeling Chemical Processing in Cloud Droplets
512 and Wet Aerosol Particles, ACS Symp. Ser., 1299, 327−345, 2018b.
513 Feng, T., Bei, N. F., Zhao, S. Y., Wu, J. R., Li, X., Zhang, T., Cao, J. J., Zhou, W. J., Li,
514 G. H.: Wintertime nitrate formation during haze days in the Guanzhong basin,
515 China: a case study, Environ. Pollut. 243, 1057–1067, 2018.
516 Fountoukis, C., Nenes, A.: ISORROPIA II: a computationally efficient thermodynamic
517 equilibrium model for K+– Ca2+–Mg2+–NH4+ –Na+–SO42- –NO3- –Cl- – H2O
518 aerosols, Atmos. Chem. Phys. 7, 4639–4659, 2007.
519 Fu, X., Wang, S. X., Chang, X., Cai, S. Y., Xing, J., Hao, J. J.: Modeling analysis of

https://doi.org/10.5194/acp-2020-760
Preprint. Discussion started: 31 August 2020


Atmospheric Chemistry and Physics Discussions

520 secondary inorganic aerosols over China: pollution characteristics, and
521 meteorological and dust impacts, Sci. Rep-UK. 6 (1), 35992, 2016.
522 Gao, M., Carmichael, G. R., Wang, Y. S., Ji, D. S., Liu, Z. R., Wang, Z. F.: Improving
523 simulations of sulfate aerosols during winter haze over northern China: the
524 impacts of heterogeneous oxidation by NO2, Front. Environ. Sci. Eng. 10 (5).,
525 2016.
526 Gao, M., Han, Z. W., Liu, Z. R., Li, M., Xin, J. Y., Tao, Z. N., Li, J. W., Kang, J. E.,
527 Huang, K., Dong, X. Y., Zhuang, B. L., Li, S., Ge, B. Z, Wu, Q. Z., Cheng, Y. F.,
528 Wang, Y. S., Lee, H. J., Kim, C. H., Fu, J. S., Wang, T. J., Chin, M., Woo, J. H.:
529 Air quality and climate change, Topic 3 of the Model Inter-Comparison Study for
530 Asia Phase III (MICS-Asia III) - Part 1: Overview and model evaluation, Atmos.
531 Chem. Phys., 18, 4859–4884, https://doi.org/10.5194/acp-18-4859-2018, 2018.
532 Ge, X. L., He, Y. N., Sun, Y. L., Xu, J. Z., Wang, J. F., Shen, Y. F., and Chen, M. D.:
533 Characteristics and Formation Mechanisms of Fine Particulate Nitrate in Typical
534 Urban Areas in China, Atmosphere, 8, 62, https://doi.org/10.3390/atmos8030062,
535 2017.
536 Grell, G. A., Dezső, D.: A generalized approach to parameterizing convection
537 combining ensemble and data assimilation techniques, Geophys. Res. Lett., 29,
538 1693, 2002.
539 Grell, G.A., Peckham, S.E., Schmitz, R., Mckeen, S.A., Frost, G., Skamarock, W.C.,
540 Eder, B.: Fully coupled “online” chemistry within the WRF model, Atmos.
541 Environ., 39 (37), 6957–6975, 2005.

https://doi.org/10.5194/acp-2020-760
Preprint. Discussion started: 31 August 2020


Atmospheric Chemistry and Physics Discussions

542 Gultepe, I., Müller, M. D., and Boybeyi, Z.: A New Visibility Parameterization for
543 Warm-Fog Applications in Numerical Weather Prediction Models, J. Appl.
544 Meteorol. Climatol., 45, 1469–1480, https://doi.org/10.1175/jam2423.1, 2006.
545 Guo, H., Weber, R. J., and Nenes, A.: High levels of ammonia do not raise fine particle
546 pH sufficiently to yield nitrogen oxide-dominated sulfate production, Sci. Rep.-
547 UK, 7, 12109, https://doi.org/10.1038/s41598-017-11704-0, 2017.
548 Harris, E., Sinha, B., van Pinxteren, D., Tilgner, A., Fomba, K. W., Schneider, J., Roth,
549 A., Gnauk, T., Fahlbusch, B., Mertes, S., Lee, T., Collett, J., Foley, S.: Borrmann,
550 S.; Hoppe, P.; Herrmann, H. Enhanced Role of Transition Metal Ion Catalysis
551 During In-Cloud Oxidation of SO2, Science, 340, 727−730, 2013.
552 Hong L., Zhu B., Yu X. N., Shi S. S., Che K., Xia L.: Chemical composition of dew
553 water at a suburban site in Nanjing, China, during the 2016–2017 winter, Atmos.
554 Environ., 211, 226 – 233, 2019.
555 Hong, S. Y., Noh, Y., Dudhia, J.: A new vertical diffusion package with an explicit
556 treatment of entrainment processes, Mon. Weather Rev., 134 (9), 2318, 2006.
557 Huang, R. J., Zhang, Y., Bozzetti, C., Ho, K. F., Cao, J. J., Han, Y., Daellenbach, K. R.,
558 Slowik, J. G., Platt, S. M., Canonaco, F., Zotter, P., Wolf, R., Pieber, S. M., Bruns,
559 E. A., Crippa, M., Ciarelli, G., Piazzalunga, A., Schwikowski, M., Abbaszade, G.,
560 SchnelleKreis, J., Zimmermann, R., An, Z., Szidat, S., Baltensperger, U., Haddad,
561 I. E., and Prevot, A. S. H.: High secondary aerosol contribution to particulate
562 pollution during haze events in China, Nature, 514, 218–222,
563 10.1038/nature13774, 2014.

https://doi.org/10.5194/acp-2020-760
Preprint. Discussion started: 31 August 2020

Atmospheric Chemistry and Physics Discussions

564 Jacob, D. J.: Heterogeneous chemistry and tropospheric ozone. Atmos. Environ., 34,
565 2131–2159, 2000.
566 Jia, X. C., Quan, J. N., Zheng, Z. Y., Liu, X. G., Liu, Q., He, H., Liu, Y. G.: Impacts of
567 anthropogenic aerosols on fog in North China Plain, J. Geophys. Res. Atmos., 124,
568 252–265. https://doi.org/10.1029/2018JD029437, 2019.
569 Kay, J. E., Hillman, B. R., Klein, S. A., Zhang, Y., Medeiros, B., Pincus, R., et al.:
570 Exposing global cloud biases in the Community Atmosphere Model (CAM) using
571 satellite observations and their corresponding instrument simulators, J. Clim.,
572 25(15), 5190–5207. https://doi.org/10.1175/jcli-d-11-00469.1, 2012.
573 Khain, A., Leung, L. R., Lynn, B., Ghan, S.: Effects of aerosols on the dynamics and
574 microphysics of squall lines simulated by spectral bin and bulk parameterization
575 schemes, J. Geophys. Res. Atmos., 114, D22203.
576 https://doi.org/10.1029/2009JD011902, 2009.
577 Khanal, S., and Wang, Z.: Uncertainties in MODIS-based cloud liquid water path
578 retrievals at high latitudes due to mixed-phase clouds and cloud top height
579 inhomogeneity, J. Geophys. Res. Atmos., 123, 11,154–11,172,
580 https://doi.org/10.1029/2018JD028558, 2018.
581 Kim, P. S., Jacob, D. J., Fisher, J. A., Travis, K., Yu, K.; Zhu, L., Yantosca, R. M.,
582 Sulprizio, M. P., Jimenez, J. L., Campuzano-Jost, P., Froyd, K. D., Liao, J., Hair,
583 J. W., Fenn, M. A., Butler, C. F., Wagner, N. L., Gordon, T. D., Welti, A., Wennberg,
584 P. O., Crounse, J. D., St. Clair, J. M., Teng, A. P., Millet, D. B., Schwarz, J. P.,
585 Markovic, M. Z., Perring, A. E.: Sources, Seasonality, and Trends of Southeast US

https://doi.org/10.5194/acp-2020-760
Preprint. Discussion started: 31 August 2020


Atmospheric Chemistry and Physics Discussions

586 Aerosol: An Integrated Analysis of Surface, Aircraft, and Satellite Observations
587 with the GEOS-Chem Chemical Transport Model, Atmos. Chem. Phys., 15,
588 10411−10433. O'Sullivan, D. W.; Lee, M.; Noone, B. C., 2015.
589 Li, G. H., Bei, N. F., Cao, J. J., Hu, R. J., Wang, J. R., Feng, T., Wang, Y. C., Liu, S. X.,
590 Zhang, Q., Tie, X. X., Molina, L. T.: A possible pathway for rapid growth of sulfate
591 during haze days in China, Atmos. Chem. Phys., 17, 3301–3316, 2017a.
592 Li, J., Chen, X. S., Wang, Z. F., Du, H. Y., Yang, W. Y., Sun, Y. L., Hu, B., Li, J. J.,
593 Wang, W., Wang, T., Fu, P. Q., Huang, H. L.: Radiative and heterogeneous
594 chemical effects of aerosols on ozone and inorganic aerosols over East Asia, Sci.
595 Total Environ., 622–623, 1327–1342, 2018a.
596 Li, L., Hoffmann, M. R., and Colussi, A. J.: Role of nitrogen dioxide in the production
597 of sulfate during Chinese haze-aerosol episodes, Environ. Sci. Technol., 52, 2686–
598 2693, https://doi.org/10.1021/acs.est.7b05222, 2018b.
599 Li, M., Zhang, Q., Kurokawa, J.-i., Woo, J.-H., He, K. B., Lu, Z. F., Ohara, T., Song, Y.,
600 Streets, D. G., Carmichael, G. R., Cheng, Y.F., Hong, C. P., Huo, H., Jiang, X. J.,
601 Kang, S., Liu, F., Su, H., Zheng, B.: MIX: a mosaic Asian anthropogenic emission
602 inventory under the international collaboration framework of the MICS-Asia and
603 HTAP, Atmos. Chem. Phys. 17, 935–963, 2017b.
604 Li, Z. Q., Guo, J. P., Ding, A. J., Liao, H., Liu, J. J., Sun, Y. L., Wang, T. J., Xue, H. W.,
605 Zhang, H. S., and Zhu, B.: Aerosol and boundary-layer interactions and impact on
606 air quality, Natl. Sci. Rev., 4, 810-833, https://doi.org/10.1093/nsr/nwx117, 2017c.
607 Liu, M. X., Song, Y., Zhou, T., Xu, Z. Y., Yan, C. Q., Zheng, M., Wu, Z. J., Hu, M., Wu,

https://doi.org/10.5194/acp-2020-760
Preprint. Discussion started: 31 August 2020


Atmospheric Chemistry and Physics Discussions

608 Y. S., and Zhu, T.: Fine particle pH during severe haze episodes in northern China,
609 Geophys. Res. Lett., 44, 1–9, https://doi.org/10.1002/2017GL073210, 2017.
610 Liu, P. F., Ye, C., Xue, C. Y., Zhang, C. L., Mu, Y. J., and Sun, X.: Formation
611 mechanisms of atmospheric nitrate and sulfate during the winter haze pollution
612 periods in Beijing: gas-phase, heterogeneous and aqueous-phase chemistry, Atmos.
613 Chem. Phys., 20, 4153–4165, https://doi.org/10.5194/acp-20-4153-2020, 2020a.
614 Liu, T., Clegg, S. L., Abbatt, J. P. D.: Fast oxidation of sulfur dioxide by hydrogen
615 peroxide in deliquesced aerosol particles, Proc. Natl Acad. Sci. USA. 117, 1354–
616 1359, 2020b.
617 Liu, Y. H., Lu, K. D., Li, X., Dong, H. B., Tan, Z. F., Wang, H. C., Zou, Q., Wu, Y. S.,
618 Zeng, L.M., Hu, M., Min, K.-E., Kecorius, S., Wiedensohler, A., and Zhang, Y. H.:
619 A comprehensive model test of the hono sources constrained to field
620 measurements at rural north china plain, Environ, Sci. Technol., 53, 3517−3525,
621 2019.
622 Lowe, D., Archer-Nicholls, S., Morgan, W., Allan, J., Utembe, S., Ouyang, B., Aruffo,
623 E., Le Breton, M., Zaveri, R. A., Di Carlo, P., Percival, C., Coe, H., Jones, R.,
624 McFiggans, G.: WRF-Chem model predictions of the regional impacts of N2O5
625 heterogeneous processes on night-time chemistry over north-western Europe,
626 Atmos. Chem. Phys. 15, 1385–1409. https://doi.org/10.5194/acp-15-1385-404
627 2015, 2015.
628 Lu, C. S.; Niu, S. J.; Tang, L. L.; Lv, J. J.; Zhao, L. J.; Zhu, B. Chemical composition
629 of fog water in Nanjing area of China and its related fog microphysics, Atmos.

https://doi.org/10.5194/acp-2020-760
Preprint. Discussion started: 31 August 2020


Atmospheric Chemistry and Physics Discussions

630 Res., 97, 47−69, 2010.

631 Luo, G., Yu, F., and Schwab, J.: Revised treatment of wet scavenging processes
632 dramatically improves GEOS-Chem 12.0.0 simulations of surface nitric acid,
633 nitrate, and ammonium over the United States, Geosci. Model Dev., 12, 3439-3447,
634 https://doi.org/640 10.5194/gmd-12-3439-2019, 2019.

635 Ma, X. Y, Sha, T., Wang, J. Y., Jia, H. L., Tian, R.: Investigating impact of emission
636 inventories on PM2.5 simulations over North China Plain by WRF-Chem, Atmos.
637 Environ. 195, 125–140, 2018.

638 Ma, X., Salzen, K.V.: Dynamics of the sulphate aerosol size distribution on a global
639 scale, J. Geophys. Res. Atmos. 111 (D8), 2006.

640 McDuffie, E. E., Fibiger, D. L., Dube, W. P., Lopez-Hilfiker, F., Lee, B. H., Thornton,
641 J. A., Shah, V., Jaegle, L., Guo, H., Weber, R. J., Reeves, J. M., Weinheimer, A. J.,
642 Schroder, J. C., Campuzano-Jost, P., Jimenez, J. L., Dibb, J. E., Veres, P., Ebben,
643 C., Sparks, T. L., Wooldridge, P. J., Cohen, R. C., Hornbrook, R. S., Apel, E. C.,
644 Campos, T., Hall, S. R., Ullmann, K., and Brown, S. S.: Heterogeneous N2O5
645 Uptake During Winter: Aircraft Measurements During the 2015 WINTER
646 Campaign and Critical Evaluation of Current Parameterizations, J. Geophys. Res.-
647 Atmos., 123, 4345-4372, https://doi.org/10.1002/2018JD028336, 2018.

648 Min Q., Joseph E., Lin Y., Min L., B. Yin, Daum P. H., Kleinman L. I., Wang J., and
649 Lee Y.-N.: Comparison of MODIS cloud microphysical properties with in-situ
650 measurements over the Southeast Pacific, Atmos. Chem. Phys., 12, 11261–11273,
651 doi:10.5194/acp-12-11261-2012, 2012.

https://doi.org/10.5194/acp-2020-760
Preprint. Discussion started: 31 August 2020


Atmospheric Chemistry and Physics Discussions

652 Mlawer, Eli. J., Steven. J. Taubman, Patrick. D. Brown, M. J. Iacono, and S. A. Clough.:
653 Radiative transfer for inhomogeneous atmospheres: RRTM, a validated
654 correlated–k model for the longwave, J. Geophys. Res., 102, 16663–16682.
655 doi:10.1029/97JD00237, 1997.
656 Moch, J. M., Dovrou, E., Mickley, L. J., Keutsch, F. N., Cheng, Y., Jacob, D. J., Jiang,
657 J.K., Li, M., Munger, J. W., Qiao, X.H., and Zhang, Q.: Contribution of
658 hydroxymethane sulfonate to ambient particulate matter: A potential explanation
659 for high particulate sulfur during severe winter haze in Beijing, Geophysical
660 Research Letters, 45, 11,969–11,979. https://doi.org/10.1029/2018GL079309,
661 2018.
662 Mueller, S. F., Bailey, E. M., Cook, T. M., & Mao, Q.: Treatment of clouds and the
663 associated response of atmospheric sulfur in the Community Multiscale Air
664 Quality (CMAQ) modeling system, Atmos. Environ., 40(35), 6804–6820.
665 https://doi.org/10.1016/j.atmosenv.2006.05.069, 2006.
666 Pye Havala O. T., Nenes A., Alexander B., Ault A. P., Barth M. C., Clegg S. L., Collett
667 Jr. J. L., Fahey K. M., Hennigan C. J., Herrmann H., Kanakidou M., Kelly J. T.,
668 Ku I-T., McNeill V. F., Riemer N., Schaefer T., Shi G. L., Tilgner A., Walker J. T.,
669 Wang T., Weber R., Xing J., Zaveri R.l A., and Zuend A.: The acidity of
670 atmospheric particles and clouds, Atmos. Chem. Phys., 20, 4809–4888,
671 https://doi.org/10.5194/acp-20-4809-2020, 2020.
672 Qin, Y. S., Liu, D. Y., Yin, Y. Y., Li, L.: Analysis of chemical characteristics in fog water
673 and pollutant source in Nanjing, Environ. Chem. 30 (4), 816–824, 2011. (in

https://doi.org/10.5194/acp-2020-760
Preprint. Discussion started: 31 August 2020

674 Chinese)

675 Qu, Z., Henze, D. K., Theys, N., Wang, J., and Wang, W.: Hybrid Mass Balance/4D-
676 Var Joint Inversion of NOx and SO2 Emissions in East Asia, J. Geophys. Res.-
677 Atmos., 124, 8203-8224, https://doi.org/10.1029/2018JD030240, 2019.

678 Rasch, P. J., Barth, M. C., Kiehl, J. T., Schwartz, S. E., Benkovitz, C. M.: A description
679 of the global sulfur cycle and its controlling processes in the national center for
680 atmospheric research community climate model, version 3, J. Geophys. Res.-
681 Atmos., 105(D1), 1367, 2000.

682 Richards J. A.: Remote Sensing Digital Image Analysis, Springer, New York, NY, USA,
683 doi:10.1007/978-3-642-30062-2, 2013.

684 Sarwar G., Simon H., Bhave P., Yarwood G.: Examining the impact of heterogeneous
685 nitryl chloride production on air quality across the United States, Atmos. Chem.
686 Phys., 12, 6455–6473, www.atmos-chem-phys.net/12/6455/2012/
687 doi:10.5194/acp-12-6455-2012, 2012.

688 Sarwar, G., Simon H., Xing J., Mathur R.: Importance of tropospheric ClNO2 chemistry
689 across the Northern Hemisphere, Geophys. Res. Lett., 41, 4050–4058,
690 doi:10.1002/2014GL059962, 2014.

691 Sha T., Ma X. Y., Jia H. L., Tian R., Chang Y. H., Cao F., Zhang Y. L.: Aerosol chemical
692 component: Simulations with WRF-Chem and comparison with observations in
693 Nanjing, Atmos. Environ., 218, 116982,
694 https://doi.org/10.1016/j.atmosenv.2019.116982, 2019.

695 Shao, J. Y., Chen, Q. J., Wang, Y. X., Lu, X., He, P. Z., Sun, Y. L., Shah, V., Martin, R.

https://doi.org/10.5194/acp-2020-760
Preprint. Discussion started: 31 August 2020

V., Philip, S., Song, S. J., Zhao, Y., Xie, Z. Q., Zhang, L., Alexander, B.: Heterogeneous sulfate aerosol formation mechanisms during wintertime Chinese haze events: air quality model assessment using observations of sulfate oxygen isotopes in Beijing, Atmos. Chem. Phys., 19, 6107–6123, 2019.

Sorooshian, A., Brechtel, F. J., Ervens, B., Feingold, G., Varutbangkul, V., Bahreini, R., Murphy, S., Holloway, J. S., Atlas, E. L., Anlauf, K., Buzorius, G., Jonsson, H., Flagan, R. C., and Seinfeld, J. H.: Oxalic acid in clear and cloudy atmospheres: Analysis of data from International Consortium for Atmospheric Research on Transport and Transformation 2004, J. Geophys. Res.-Atmos., 111, D23S45, https://doi.org/10.1029/2005JD006880, 2006.

Sorooshian, A., Lu, M.-L., Brechtel, F. J., Jonsson, H., Feingold, G., Flagan, R. C., and Seinfeld, J. H.: On the source of organic acid aerosol layers above clouds, Environ. Sci. Technol., 41, 4647– 4654, 2007.

Su, T., Li, Z., and Kahn, R.: Relationships between the planetary boundary layer height and surface pollutants derived from lidar observations over China: regional pattern and influencing factors, Atmos. Chem. Phys., 18, 15921-15935, https://doi.org/10.5194/acp-18-15921-2018, 2018.

Sukoriansky, S., B. Galperin, and V. Perov.: Application of a new spectral model of stratified turbulence to the atmospheric boundary layer over sea ice, Bound. Layer Meteor., 117, 231–257, doi:10.1007/s10546-004-6848-4, 2005.

Tewari, M., Chen F., Wang W., Dudhia J., LeMone M. A., Mitchell K., M. Gayno Ek, Wegiel G., J., and Cuenca R. H.: Implementation and verification of the unified

https://doi.org/10.5194/acp-2020-760
Preprint. Discussion started: 31 August 2020


Atmospheric Chemistry and Physics Discussions

718 NOAH land surface model in the WRF model. 20th conference on weather
719 analysis and forecasting/16th conference on numerical weather prediction, pp. 11–
720 15, 2004.
721 Tie X. X., Huang R. J., Cao J. J., Zhang Q., Cheng Y. F., Su H., Chang D., Pöschl U.,
722 Hoffmann T., Dusek U., Li G.H., Worsnop D. R., D. O'Dowd C.: Severe Pollution
723 in China Amplified by Atmospheric Moisture, Sci Rep., 7: 15760,
724 doi:10.1038/s41598-017-15909-1, 2017.
725 Wang J. F., Li J. Y., Ye J. H., Zhao, J., Wu Y. Z., Hu J. L., Liu D. T., Nie D. Y., Shen F.
726 Z., Huang X. P., Huang D. D., Ji D. S., Sun X., Xu W. Q., Guo J. P., Song S. J.,
727 Qin Y. M., Liu P. F., Turner J. R., Lee H. C., Hwang S., Liao H., Martin S. T.,
728 Zhang Q., Chen M. D., Sun Y. L., Ge X. L., Jacob D. J.: Fast sulfate formation
729 from oxidation of SO2 by NO2 and HONO observed in Beijing haze, Nat.
730 Commun., 11:2844, https://doi.org/10.1038/s41467-020-16683-x, 2020.
731 Wang Y. C., Chen J., Wang Q. Y., Qin Q. D., Ye J. H., Han Y. M., Li L., Zhen W., Zhi
732 Q., Zhang Y. X., Cao J. J..: Increased secondary aerosol contribution and possible
733 processing on polluted winter days in China, Environ. Int., 127, 78–84,
734 https://doi.org/10.1016/j.envint.2019.03.021, 2019.
735 Wang, G. H., Zhang, R. Y., Gomez, M. E., Yang, L. X., Zamora, M. L., Hu, M., Lin, Y.,
736 Peng, J. F., Guo, S., Meng, J. J., Li, J. J., Cheng, C. L., Hu, T. F., Ren, Y. Q., Wang,
737 X. S., Gao, J., An, Z. S., Zhou, W. J., Li, G. H., Wang, J. Y., Tian, Y. Q., Marrero-
738 Ortiz, W., Secrest, J., Du, Z. F., Zheng, J., Dongjie, S., Zeng, L., Shao, M., Wang,
739 W. G., Huang, Y., Wang, Y., Zhu, Y. J., Li, Y. X., Hu, J. X., Pan, B., Cai, L., Cheng,

https://doi.org/10.5194/acp-2020-760
Preprint. Discussion started: 31 August 2020

740 Y. T., Ji, Y. M., Zhang, F., Rosenfeld, D., Liss, P. S., Duce, R. A., Kolb, C. E.,
741 Molinax, M.J.: Persistent sulfate formation from London Fog to Chinese haze,
742 Proc. Natl. Acad. Sci. U.S.A., 48 (113), 13630–13635, 2016.
743 Wang, J., S. Park, J. Zeng, K. Yang, S. Carn, N. Krotkov, and A. Omar, Modeling of
744 2008 Kasatochi volcanic sulfate direct radiative forcing: assimilation of OMI SO2
745 plume height data and comparison with MODIS and CALIOP observations,
746 Atmospheric Chemistry and Physics, 13, 1895-1912, 2013.
747 Wang, Y. S., Yao, L., Wang, L. L., Liu, Z. R., Ji, D. S., Tang, G. Q., Zhang, J. K., Sun,
748 Y. L., Hu, B., and Xin, J. Y.: Mechanism for the formation of the January 2013
749 heavy haze pollution episode over central and eastern China, Sci. China Earth Sci.,
750 57, 14–25, https://doi.org/10.1007/s11430-013-4773-4, 2013.
751 Wang, Y. X., Zhang, Q. Q., Jiang, J. K., Zhou, W., Wang, B. Y., He, K. B., Duan, F. K.,
752 Zhang, Q., Philip, S., and Xie, Y. Y.: Enhanced sulfate formation during China's
753 severe winter haze episode in January 2013 missing from current models, J.
754 Geophys. Res.-Atmos., 770 119, 10425-10440,
755 https://doi.org/10.1002/2013JD021426, 2014.
756 Weber, R. J., Guo, H., Russell, A. G., and Nenes, A.: High aerosol acidity despite
757 declining atmospheric sulfate concentrations over the past 15 years, Nat. Geosci.,
758 9, 282–285, https://doi.org/10.1038/ngeo2665, 2016.
759 Wonaschuetz, A., Sorooshian, A., Ervens, B., Chuang, P. Y., Feingold, G., Murphy, S.
760 M., de Gouw, J., Warneke, C., and Jonsson, H. H.: Aerosol and gas re-distribution
761 by shallow cumulus clouds: An investigation using airborne measurements, J.

https://doi.org/10.5194/acp-2020-760
Preprint. Discussion started: 31 August 2020


Atmospheric Chemistry and Physics Discussions

762 Geophys. Res.-Atmos., 117, D17202, https://doi.org/10.1029/2012jd018089,
763 2012.
764 Wu J. R., Bei N. F., Hu B., Liu S. X., Zhou M., Wang Q. Y., Li X., Liu L., Feng T., Liu
765 Z. R., Wang Y. C., Cao J. J., Tie X. X., Wang J., Molina L. T., and Li G. H.: Is
766 water vapor a key player of the wintertime haze in North China Plain? Atmos.
767 Chem. Phys., 19, 8721–8739, https://doi.org/10.5194/acp-19-8721-2019, 2019.
768 Xie, Y. Y., Wang, Y. X., Dong, W. H., Wright, J. S., Shen, L., Zhao, Z. J.: Evaluating
769 the response of summertime surface sulfate to hydroclimate variations in the
770 continental United States: Role of meteorological inputs in the GEOS-Chem
771 model, J. Geophys. Res. Atmos., 124. https://doi.org/10.1029/2018JD029693,
772 2019.
773 Xu, L. L., Duan, F. K., He, K. B., Ma, Y. L., Zhu, L. D., Zheng, Y. X., Huang, T., Kimoto,
774 T., Ma, T., Li, H., Ye, S., Yang, S., Sun, Z. L., and Xu, B. Y.: Characteristics of the
775 secondary water-soluble ions in a typical autumn haze in Beijing, Environ. Pollut.,
776 227, 296–305, https://doi.org/10.1016/j.envpol.2017.04.076, 2017.
777 Xue J., Yuan Z. B., Griffith S. M., Yu X., Lau Alexis K. H., and Yu J. Z.: Sulfate
778 Formation Enhanced by a Cocktail of High NOx, SO2, Particulate Matter, and
779 Droplet pH during Haze-Fog Events in Megacities in China: An Observation-
780 Based Modeling Investigation, Environ, Sci. Technol., 50, 7325−7334, doi:
781 10.1021/acs.est.6b00768, 2016.
782 Yan, W. L., Zhang, G. Z., PU, M. J., Liu, D. Y., Li, Z. H.: Chemical features and cause
783 analysis of a strong acid fog event in Nanjing, J. Nat. Disasters 22 (3), 122–129,

https://doi.org/10.5194/acp-2020-760
Preprint. Discussion started: 31 August 2020

2013. (in Chinese)

Yang, T., Sun, Y. L., Zhang, W., Wang, Z. F., Liu, X. G., Fu, P. Q., and Wang, X. Q.: Evolutionary processes and sources of high-nitrate haze episodes over Beijing, Spring, J. Environ. Sci., 54, 142–151, https://doi.org/10.1016/j.jes.2016.04.024, 2017.

Young, L. H., Li, C. H., Lin, M. Y., Hwang, B. F., Hsu, H. T., Chen, Y. C., Jung, C. R., Chen, K. C., Cheng, D. H., Wang, V. S., Chiang, H. C., Tsai, P. J.: Field performance of a semi-continuous monitor for ambient PM2.5 water-soluble inorganic ions and gases at a suburban site, Atmos. Environ., 144, 376-388, http://dx.doi.org/10.1016/j.atmosenv.2016.08.062, 2016.

Zaveri, R. A., Peters, L. K.: A new lumped structure photochemical mechanism for large-scale applications, J. Geophys. Res. Atmos. 104, 30387–30415, 1999.

Zaveri, R.A., Easter, R. C., Fast, J. D., Peters, L. K.: Model for simulating aerosol interactions and chemistry (MOSAIC), J. Geophys. Res. Atmos., 113, D13204, 2008.

Zhang, L., Chen, Y. F., Zhao, Y. H., Henze, D. K., Zhu, L. Y., Song, Y., Paulot, F., Liu, X. J., Pan, Y. P., Lin, Y., and Huang, B. X.: Agricultural ammonia emissions in China: reconciling bottom-up and top-down estimates, Atmos. Chem. Phys., 18, 339-355, https://doi.org/10.5194/acp-18-339-2018, 2018.

Zheng, B., Zhang, Q., Zhang, Y., He, K. B., Wang, K., Zheng, G. J., Duan, F. K., Ma, Y. L., Kimoto, T.: Heterogeneous chemistry: a mechanism missing in current models to explain secondary inorganic aerosol formation during the January 2013

https://doi.org/10.5194/acp-2020-760
Preprint. Discussion started: 31 August 2020

haze episode in North China, Atmos. Chem. Phys. 15, 2031–2049, 2015a.

Zheng, G. J., Duan, F. K., Su, H., Ma, Y. L., Cheng, Y., Zheng, B., Zhang, Q., Huang, T., Kimoto, T., Chang, D., Poschl, U., Cheng, Y. F., and He, K. B.: Exploring the severe winter haze in Beijing: the impact of synoptic weather, regional transport and heterogeneous reactions, Atmos. Chem. Phys., 15, 2969-2983, https://doi.org/10.5194/acp-15-2969-2015, 2015b.

https://doi.org/10.5194/acp-2020-760
Preprint. Discussion started: 31 August 2020

Atmospheric Chemistry and Physics Discussions

Table 1. Comparison of the simulated and observed meteorological parameters. (T2: 2 meters temperature (°C), RH2: 2 meters relative humidity (%), WS10: 10 meters wind speed ($m \cdot s^{-1}$), WS10: 10 meters wind speed ($m \cdot s^{-1}$)).

Variables	Obs	Mod	R	MB	RMSE
T2	11.5	11.1	0.89	-0.4	1.7
RH2	89.9	88.5	0.68	-1.4	9.7
WS10	1.6	1.5	0.47	-0.1	0.6
WD10	134.2	138.4	0.55	4.2	61.7

https://doi.org/10.5194/acp-2020-760
Preprint. Discussion started: 31 August 2020

Atmospheric Chemistry and Physics Discussions

818 Table 2 Statistics of the cumulative probability distribution of observed and simulated

819 LWP.

Probability (%)	Observation	Simulation
0-20 g m^{-2}	30	79
20-40 g m^{-2}	19	4
40-60 g m^{-2}	15	3
60-80 g m^{-2}	4	2
80-100 g m^{-2}	4	2
> 100 g m^{-2}	28	10

820

821

https://doi.org/10.5194/acp-2020-760
Preprint. Discussion started: 31 August 2020

Atmospheric Chemistry and Physics Discussions

822 Table 3. Descriptions of the model simulations.

Experiment name	Description
Control	Control simulation.
Sen_c	Only constrain the simulated LWP according to Eq. (4).
Sen_c_pH	Constrain the simulated LWP according to Eq. (4) and increase the cloud water pH by 2.

823

824

https://doi.org/10.5194/acp-2020-760
Preprint. Discussion started: 31 August 2020

Atmospheric Chemistry and Physics Discussions

825 Table 4 Summaries of the observed fog water pH during the fog events in Nanjing,

826 China.

Study time	pH in fog	Reference
December 2006	5.6	Li et al., 2008
December 2006 and December 2007	5.9	Lu et al., 2010
December 2007	5.5	Qin et al., 2011
December 2009	6.0 (radiation fog) 5.6 (advection radiation fog) 4.3 (advection fog)	Yan et al., 2013
November 2016 to January 2017	avg: 5.7, min: 5.0, max: 6.5	Hong et al., 2019

827

828

https://doi.org/10.5194/acp-2020-760
Preprint. Discussion started: 31 August 2020

Atmospheric Chemistry and Physics Discussions

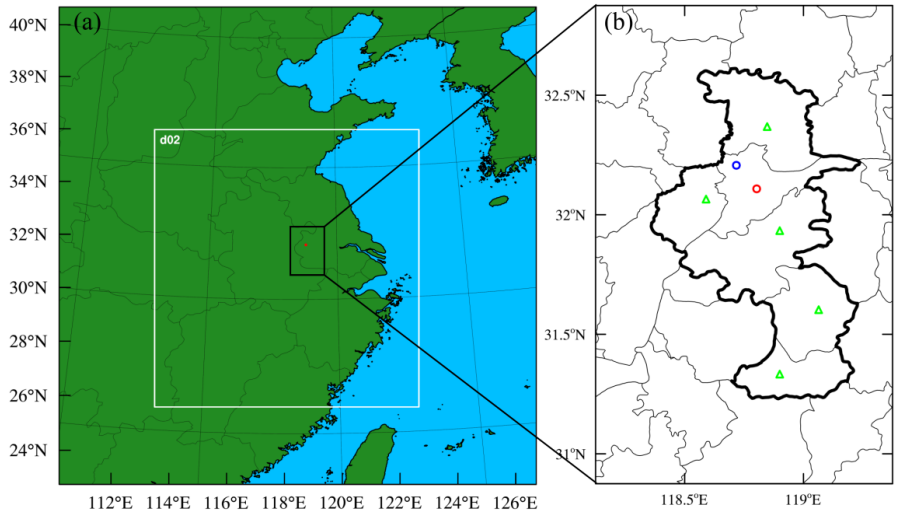

829

830 Figure 1. (a) The model domain (Solid red dot is Nanjing). (b) The location of sites with
831 in-situ measurements on meteorological variables and air pollutants (Green triangles,
832 red and blue circle denote the routine meteorological stations, Maigaoqiao air quality
833 monitoring site, and Nanjing University of Information Science & Technology
834 (NUIST), respectively).

835

https://doi.org/10.5194/acp-2020-760
Preprint. Discussion started: 31 August 2020

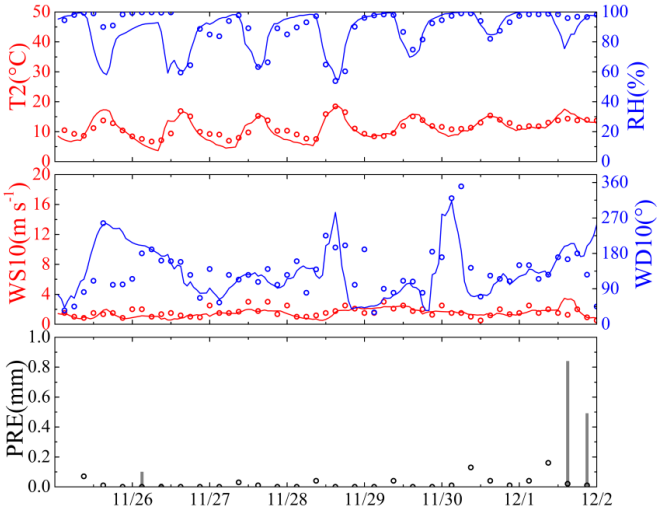

Figure 2. The performance of the simulated hourly meteorological parameters (2m temperature (T2), 2m relative humidity (RH), 10m wind speed (WS10), 10m wind direction (WD10), and 6 h accumulation precipitation (PRE)) during the haze-fog event in Nanjing. Scatters and solid lines (or columns) represent observations and simulations, respectively.

https://doi.org/10.5194/acp-2020-760
Preprint. Discussion started: 31 August 2020

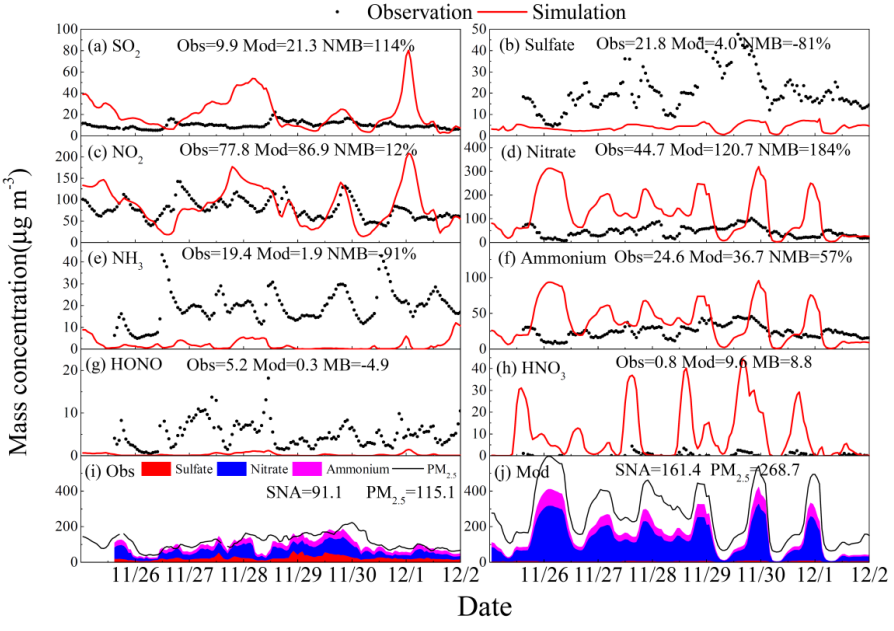

Figure 3. Time series of the simulated and observed hourly gas precursors ((a) SO_2, (c) NO_2, (e) NH_3, (g) HONO, (h) HNO_3), as well as (b) sulfate, (d) nitrate and (f) ammonium concentrations. The stacked diagram of hourly SNA and $PM_{2.5}$ concentrations from (i) observations and (j) simulations during the haze-fog event in Nanjing.

https://doi.org/10.5194/acp-2020-760
Preprint. Discussion started: 31 August 2020

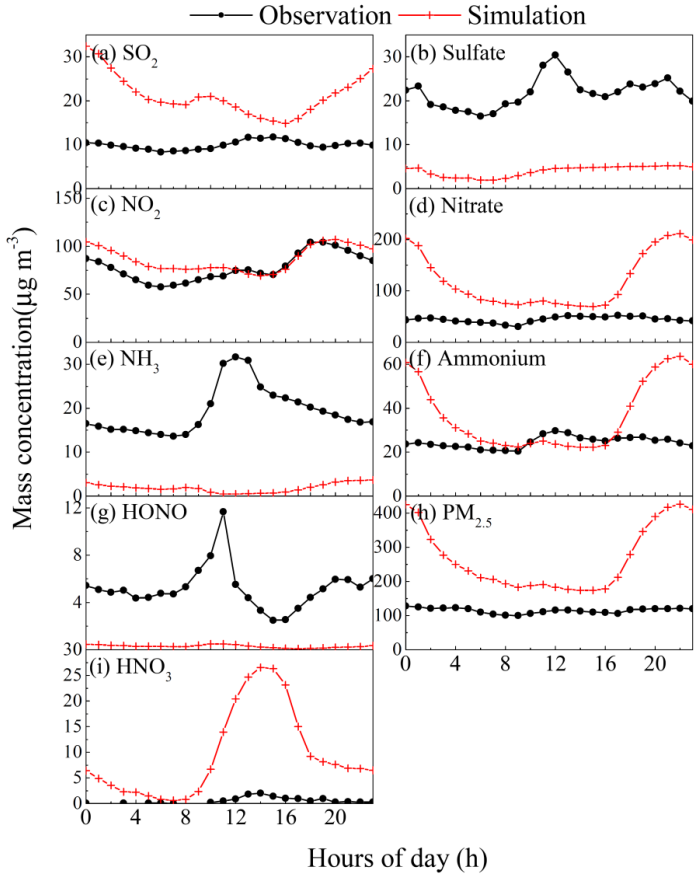

Figure 4. Diurnal cycles of the simulated and observed mass concentrations of gas precursors ((a) SO_2, (c) NO_2, (e) NH_3, (g) HONO, (i) HNO_3), as well as (b) sulfate, (d) nitrate, (f) ammonium and (h) $PM_{2.5}$ averaged during the haze-fog event in Nanjing.

https://doi.org/10.5194/acp-2020-760
Preprint. Discussion started: 31 August 2020

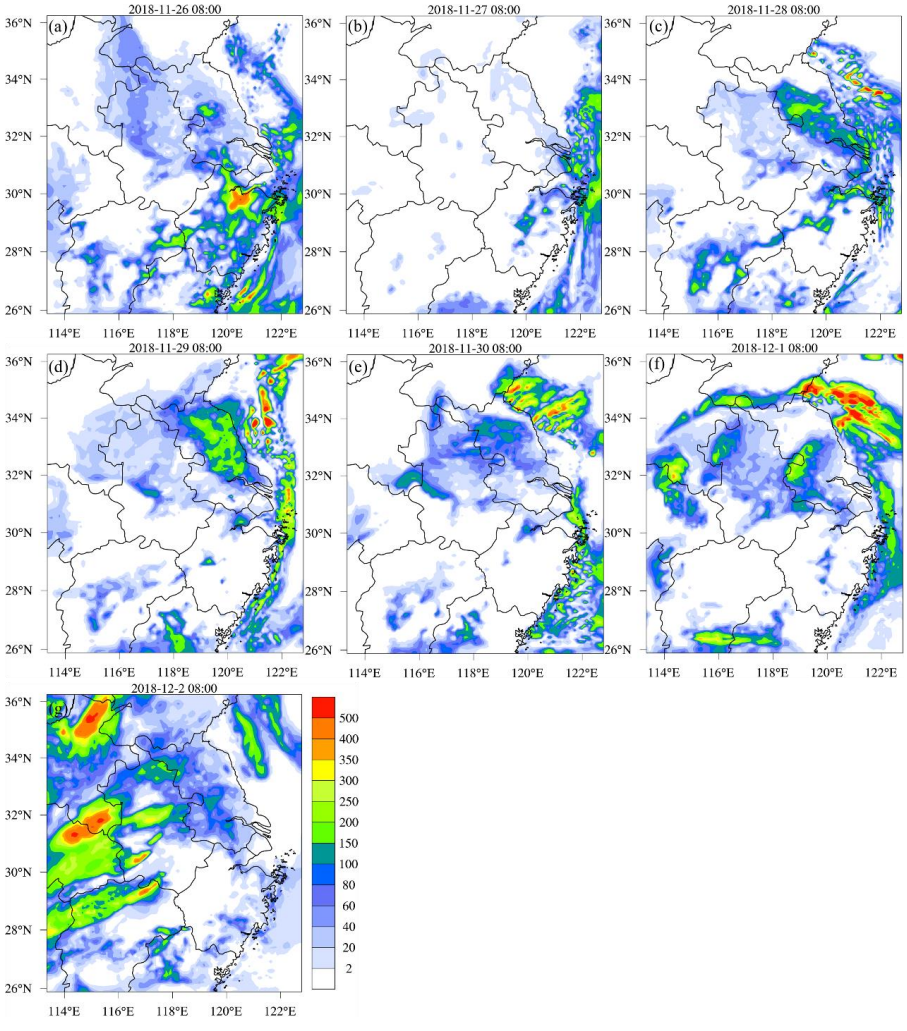

Figure 5. Distribution of the simulated liquid water path (LWP, unit: g m^{-2}) at 08:00 from 26 November to 2 December over YRD.

https://doi.org/10.5194/acp-2020-760
Preprint. Discussion started: 31 August 2020

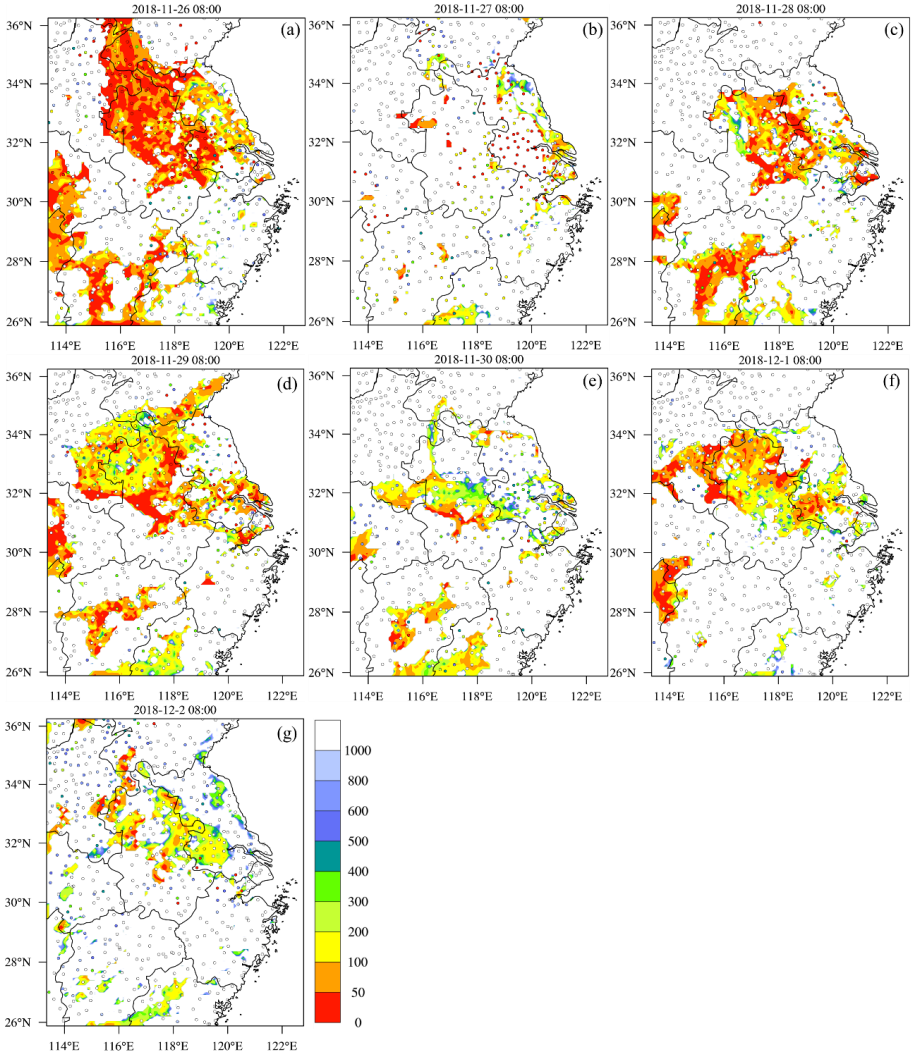

Figure 6. Distribution of the simulated and observed visibility (unit: m) at 08:00 from 26 November to 2 December over YRD. The circles represent the MICAPS observations.

https://doi.org/10.5194/acp-2020-760
Preprint. Discussion started: 31 August 2020

Atmospheric Chemistry and Physics Discussions

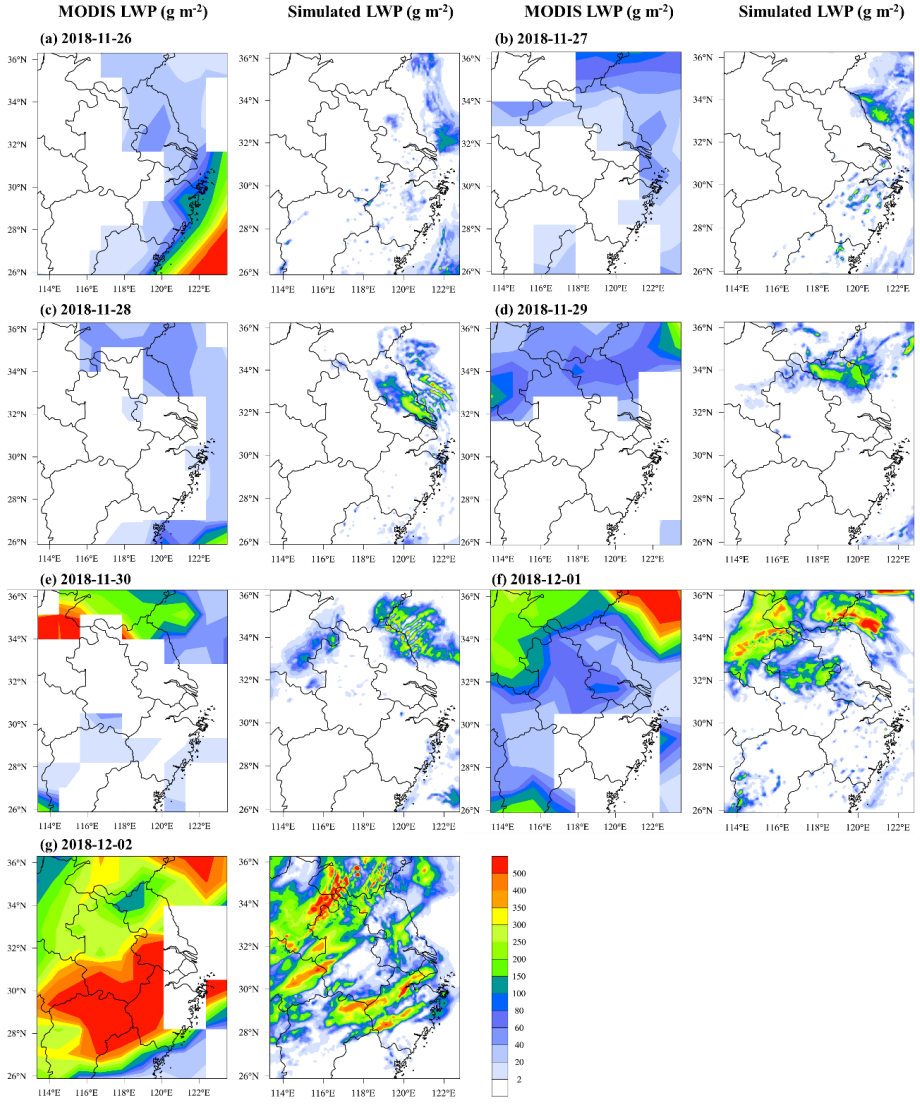

862

863 Figure 7. Distribution of LWP (unit: g m^{-2}) from the MODIS observations (columns 1

864 and 3) and simulations (columns 2 and 4) at 13:30 from 26 November to 2 December

865 over YRD.

866

https://doi.org/10.5194/acp-2020-760
Preprint. Discussion started: 31 August 2020

Atmospheric Chemistry and Physics Discussions

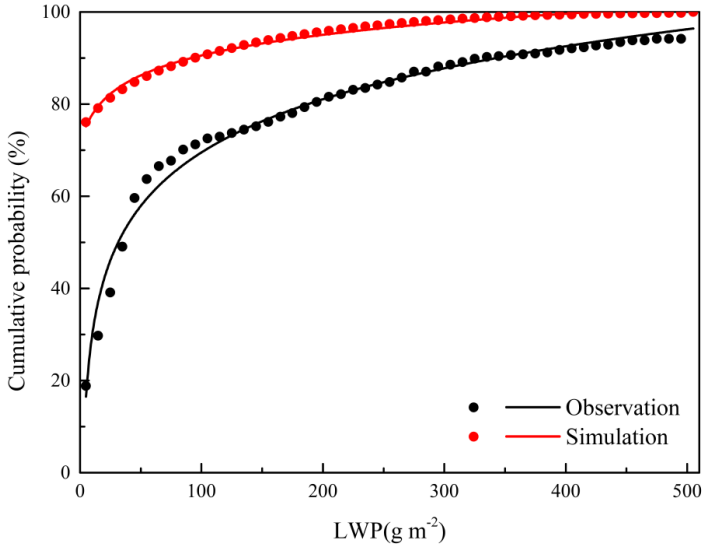

867

868 Figure 8. The cumulative probability distribution of LWP between the MODIS
869 observations and simulations. Results are based on statistics of the observed and
870 simulated daily LWP during the haze-fog event over YRD. The lines are the fitting
871 functions.

872

https://doi.org/10.5194/acp-2020-760
Preprint. Discussion started: 31 August 2020

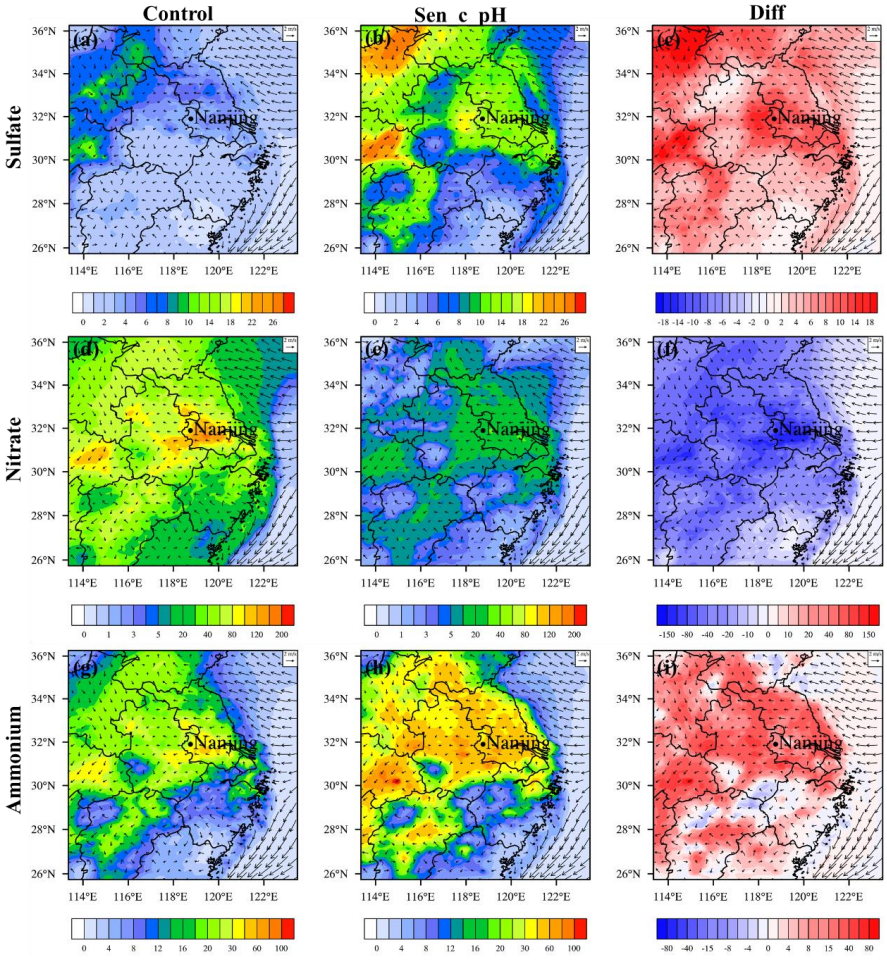

Figure 9. Distribution of the simulated sulfate, nitrate, and ammonium (SNA) in the Control run (a, d, g) and Sen_c_pH (b, e, h) simulation, and the differences of simulated SNA between the two simulations (c, f, i) during the haze-fog event over YRD. The black arrows indicate the simulated surface wind fields.

https://doi.org/10.5194/acp-2020-760
Preprint. Discussion started: 31 August 2020

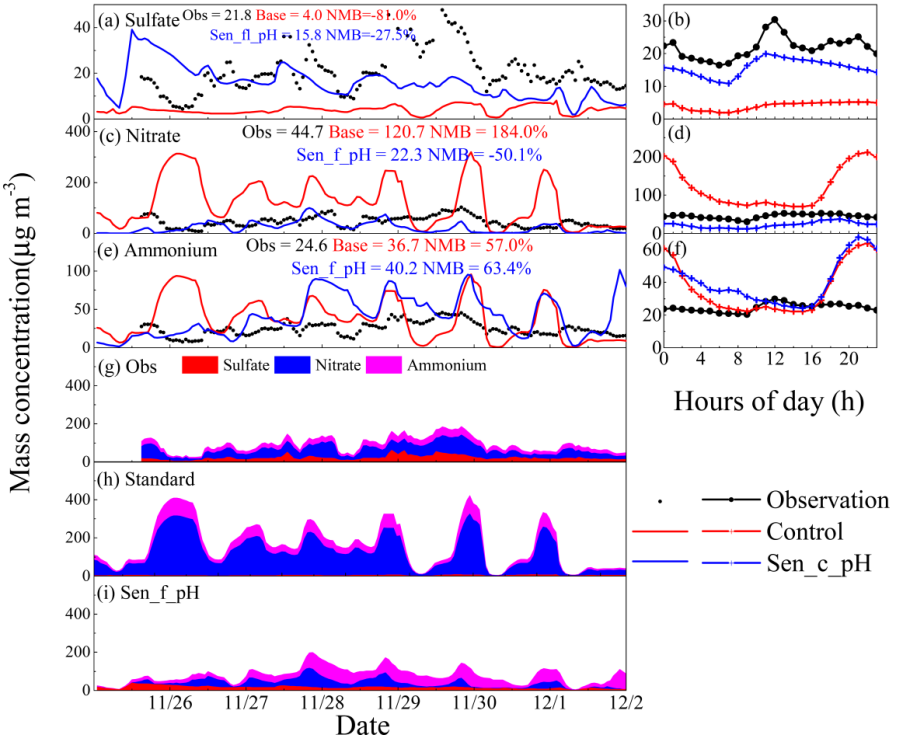

Figure 10. The hourly and diurnal variations of simulated (Control and Sen_c_pH) and observed (a, b) sulfate, (c, d) nitrate, and (e, f) ammonium concentrations. The stacked diagram of hourly SNA concentrations from (g) observations, (h) Control run, and (i) Sen_c_pH simulations during the haze-fog event in Nanjing.

https://doi.org/10.5194/acp-2020-760
Preprint. Discussion started: 31 August 2020

Atmospheric Chemistry and Physics Discussions

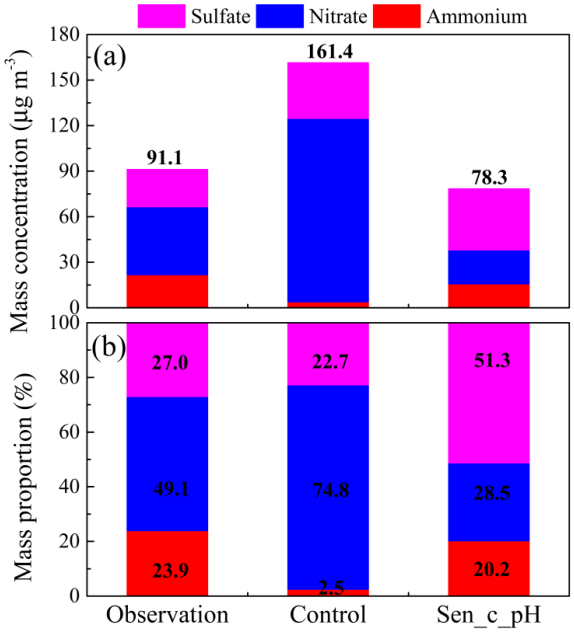

885

886 Figure 11. (a) The average mass concentrations and (b) proportion of the observed and

887 simulated (Control and Sen_c_pH) SNA during the haze-fog event in Nanjing.

888